J. Astron. Space Sci. 23(2), 91–96 (2006)

RED GIANT BRANCH OF THE METAL POOR GLOBULAR CLUSTERS: I. BUMP, TIP, AND DISTANCE FROM NEAR INFRARED PHOTOMETRY

Y.-J. Sohn†, J.-W. Kim, and A. Kang
Department of Astronomy, Yonsei University, Seoul 120-749, Korea
email: sohnyj@yonsei.ac.kr

(Received April 4, 2006; Accepted May 8, 2006)

ABSTRACT

We use near-infrared observations of eight selected Galactic globular clusters to estimate their distances by comparing the observed and theoretically predicted K magnitudes of the red giant branch bumps and tips. The K magnitude levels of the RGB bump and tip have been measured from the luminosity function of the selected RGB stars in the clusters. Theoretical absolute M_K magnitudes of the RGB bump and tip are taken from the Yonsei-Yale isochrones. Comparing the observed apparent K magnitude with the derived absolute M_K magnitude, we calculate the distance moduli of the clusters. We discuss the dependency of the derived distance modulus on the cluster age and the uncertainty of the distance measurement from the near-infrared photometry of the RGB bump and tip.

Keywords : RGB bump, RGB tip, distance, globular clusters, near-infrared photometry

1. INTRODUCTION

The magnitude levels of the red giant branch (RGB) bump and the RGB tip on the luminosity function (LF) of the RGB stars in globular clusters contain crucial astrophysical significance of the low-mass stellar evolution and the cosmic distance scale of the system. The RGB bump is an evolutionary feature during the post main-sequence evolution of low mass stars at the hydrogen-burning shell stage after the first dredge-up in a star. When the convective envelope penetrates deeply enough into the narrow hydrogen burning shell, an hesitation by a change in evolutionary rate is expected at some level along the RGB. This yields an RGB bump on the LF of RGB stars in a globular cluster. The RGB tip marks the helium ignition in the degenerate He core of low-mass stars. The observable of the RGB tip is the sharp cut-off occurring at the bright end of the LF of the RGB stars in a cluster.

The physical origin of the RGB bump was first pointed out by Thomas (1967) and Iben (1968). Since King et al. (1985) first identified the RGB bump from the observation of 47 Tuc, the detection of the RGB bump from LFs has been the subject of many studies (e.g., Fusi Pecci et al. 1990, Ferraro et al. 1999, Cho & Lee 2002, Valenti et al. 2005, and references therein). Meanwhile, the luminosity of the RGB tip is weakly sensitive to the metallicity of the stellar population especially in I band, and the RGB tip is now recognized as a mature and widely used standard candle for estimating the

†corresponding author

Table 1. The adopted K magnitudes of the RGB bump and tip, the metallicity, and the reddening value of the sample clusters.

Name	K^{Bump}	K^{Tip}	[Fe/H]	E(B-V)
M3	13.22 ± 0.05	8.83 ± 0.05	-1.34	0.01
NGC 5897	13.46 ± 0.08	9.62 ± 0.08	-1.59	0.09
M13	12.47 ± 0.05	8.23 ± 0.05	-1.39	0.02
NGC 6541	12.50 ± 0.04	8.42 ± 0.04	-1.62	0.14
NGC 6642	13.07 ± 0.05	8.36 ± 0.05	-1.08	0.41
NGC 6681	13.14 ± 0.09	8.63 ± 0.09	-1.27	0.07
NGC 6717	12.94 ± 0.08	9.02 ± 0.08	-1.10	0.22
NGC 6723	13.07 ± 0.05	8.63 ± 0.05	-0.93	0.05

distance to galaxies of any morphological type (Lee et al. 1993, Madore & Freedman 1995, Ferrarese et al. 2000a,b, Bellazzini et al. 2001, Walker 2003).

We note, however, that measuring the magnitudes of RGB bump and tip of a globular cluster in optical bands is hampered by difficulties such as foreground reddening, internal differential reddening, background crowding by faint main-sequence stars, and foreground contamination. These complications introduced in the optical band photometry can be reduced by observing at infrared wavelengths. Indeed, the extinction in K band is only $\sim$1/10 that in V band (Rieke & Lebofsky 1985). In addition, near-infrared photometry offers an advantage in studying the RGB population, because of its high sensitivity to low temperature. Cho & Lee (2002) measured the absolute M_K magnitudes of the RGB bump for 16 globular clusters and suggested that the correlation between the M_K of the RGB bump and the metallicity can be used to determine distance moduli of globular clusters with an uncertainty of $\Delta M_K \approx \pm 0.24$ mag at a given metallicity. Recently, Ferraro et al. (2000) and Valenti et al. (2004) presented a new calibration of the relation between the brightness of the RGB bump and the RGB tip in the K magnitude and the cluster metallicity.

In this paper, we use the observed K magnitudes of the RGB bump and tip of eight selected globular clusters in the Galactic bulge and halo in order to estimate their distances. The apparent K magnitudes of the RGB bump and tip of the clusters are described in Sec. 2. In Sec. 3 we present the absolute magnitudes of the RGB bump and tip predicted by the Yonsei-Yale isochrones. The calculated distances of the sample clusters are presented in Sec. 4. Results are summarized in Sec. 5.

2. THE APPARENT K MAGNITUDE

In our earlier work of Kim et al. (2006), we presented the details of our near-infrared photometry work of a sample of five metal-poor bulge clusters (NGC 6541, NGC 6642, NGC 6681, NGC 6717, and NGC 6723) and three halo clusters (M3, NGC 5897, and M13). Specifically, we investigated the morphological properties of the stellar populations in the near-infrared color-magnitude diagrams (CMDs) of the sample clusters. Several photometric parameters to describe the RGB shape, and magnitudes of the RGB bump and tip were determined from the near-infrared CMDs, and we found the derived parameters follow the previous empirical calibrations to the cluster's metallicity (e.g., Ferraro et al. 2000, Valenti et al. 2004).

The apparent K magnitudes of the RGB bump and tip were determined from the LF of each cluster using a procedure similar to that of Kim et al. (2006). First, RGB stars within a 2σ deviation

Table 2. Theoretical prediction of the absolute M_K magnitudes of the RGB bump and tip with respect to metallicity and age from the Yonsei-Yale isochrones.

	Bump					Tip			
[Fe/H]	7 Gyr	10 Gyr	12 Gyr	15 Gyr	[Fe/H]	10 Gyr	12 Gyr	14 Gyr	16 Gyr
0.169	-1.107	-0.884	-0.721	-0.566	0.000	-6.905	-6.946	-6.968	-6.989
-0.424	-1.181	-0.987	-0.910	-0.723	-0.300	-6.738	-6.795	-6.829	-6.846
-0.490	-1.421	-1.198	-1.106	-1.000	-0.600	-6.587	-6.644	-6.688	-6.708
-0.650	-1.588	-1.386	-1.291	-1.177	-0.900	-6.412	-6.449	-6.470	-6.492
-0.898	-1.774	-1.594	-1.499	-1.377	-1.200	-6.208	-6.235	-6.254	-6.276
-1.505	-2.291	-2.118	-2.015	-1.878	-1.500	-5.990	-6.022	-6.052	-6.070
-1.904	-2.619	-2.462	-2.369	-2.266	-1.800	-5.764	-5.812	-5.854	-5.870
-2.507	-2.985	-2.827	-2.740	-	-2.100	-5.586	-5.643	-5.690	-5.706
-3.507	-3.433	-	-	-	-2.400	-5.463	-5.519	-5.564	-5.578
-	-	-	-	-	-2.700	-5.372	-5.423	-5.462	-5.478
-	-	-	-	-	-3.000	-5.297	-5.344	-5.381	-5.395

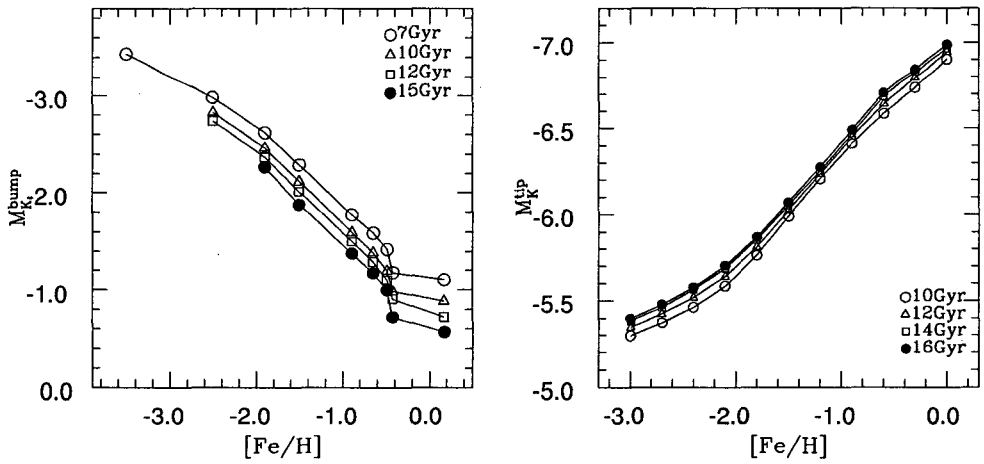

Figure 1. The absolute M_K magnitudes of the RGB bump (left) and tip (right) as a function of metallicity [Fe/H].

of the mean color for a given 0.25 magnitude bin were included to the RGB sample. A 2σ rejection procedure was then iterated until the mean values of magnitude and color are stable at constant values to avoid contamination from the other stellar populations. The LFs of each cluster were constructed from the selected RGB stars, and the RGB bump was defined at a significant peak in the differential LF and a corresponding slope break in the cumulative LF for each cluster. Meanwhile, the magnitude of the RGB tip was determined by measurements of the brightness of the brightest stars and a sharp cut-off occurring at the bright end of the LF of the RGB stars. The resulting K magnitudes for each cluster are shown in Table 1. Errors in the apparent K magnitude are the measurement errors in the LFs with a variable magnitude bin.

Table 3. Derived M_K magnitudes of the RGB bump and tip with respect to the cluster age at a given metallicity for each cluster.

	age (Gyr)	M3	N5897	M13	N6541	N6642	N6681	N6717	N6723
M_K^{bump}	7	-2.150	-2.361	-2.193	-2.386	-1.929	-2.091	-1.946	-1.801
	10	-1.976	-2.191	-2.019	-2.217	-1.751	-1.915	-1.768	-1.622
	12	-1.875	-2.090	-1.917	-2.117	-1.654	-1.815	-1.671	-1.526
	15	-1.742	-1.961	-1.783	-1.990	-1.527	-1.684	-1.544	-1.403
M_K^{tip}	10	-6.106	-5.922	-6.070	-5.900	-6.290	-6.157	-6.276	-6.392
	12	-6.136	-5.959	-6.100	-5.938	-6.321	-6.185	-6.306	-6.428
	14	-6.160	-5.993	-6.126	-5.973	-6.340	-6.207	-6.326	-6.448
	16	-6.180	-6.010	-6.146	-5.990	-6.362	-6.228	-6.348	-6.470

3. THE ABSOLUTE M_K MAGNITUDE FROM YONSEI-YALE ISOCHRONES

3.1 Adopted metallicity and reddening

As Kim et al. (2006), we adopted metallicities of the five metal-poor sample globular clusters (M3, NGC 5897, M13, NGC 6681, and NGC 6717) from Ferraro et al. (1999). The metallicities of the other three clusters (NGC 6541, NGC 6642, and NGC 6723) were estimated by transforming the value in Zinn (1985) into Carreta & Gratton (1997) scale as Ferraro et al. (2000). The adopted metallicities are listed in column 4 of Table 1, and we use them for the current study. We also use the reddening value of each cluster adopted in Kim et al. (2006), from which we estimate A_K with A_K/E(B-V)=0.367 (Schlegel et al. 1998).

3.2 Absolute M_K magnitudes

The theoretical prediction of the absolute M_K magnitudes of the RGB bump and tip is estimated by the Yonsei-Yale isochrones (Kim et al. 2002, Yi et al. 2003) for the $\alpha-$elements enhancement factor of 0.3. Table 2 and Figure 1 show the theoretical prediction of the M_K magnitudes of the RGB bump and tip with respect to the cluster metallicity and age. It is apparent from Figure 1 that the RGB bump and tip magnitudes of M_K are a strong function of metallicity and a weak function of age of a cluster. The RGB bump moves to fainter location with increasing cluster metallicity and age, while the RGB tip moves to brighter location with increasing metallicity and age of a cluster.

The absolute M_K magnitudes of the RGB bump and tip at a given metallicity for each cluster are calculated by applying the polynomial interpolation to the theoretical magnitude-metallicity planes in Figure 1. The metallicity of each cluster is assumed to be the adopted values in Table 1. Table 3 lists the estimated theoretical M_K magnitudes of the RGB bump and tip with respect to the cluster age at the given metallicity of each cluster.

4. DISTANCE

The distance modulus of each cluster can now be directly calculated by using the observed K magnitude, the adopted reddening value, and the derived absolute M_K magnitude of the RGB bump and tip. Table 4 lists the final distance moduli of the sample clusters with respect to the cluster ages at given metallicities. Error of the calculated distance modulus of each cluster in Table 3 only includes uncertainties in measurements of the RGB bump or tip as in Table 1.

The dependency of the distance on the cluster age is checked by comparing the calculated dis-

Table 4. Calculated distance moduli of each cluster from the RGB bump and tip with respect to the cluster age.

	age (Gyr)	M3	N5897	M13	N6541	N6642	N6681	N6717	N6723
μ_o^{bump}	7	15.37	15.79	14.66	14.83	14.85	15.21	14.81	14.85
	10	15.19	15.62	14.48	14.67	14.67	15.03	14.63	14.67
	12	15.09	15.52	14.38	14.57	14.57	14.93	14.53	14.58
	15	14.96	15.39	14.25	14.44	14.45	14.80	14.40	14.45
μ_o^{tip}	10	14.93	15.51	14.29	14.27	14.50	14.76	15.22	15.00
	12	14.96	15.55	14.32	14.31	14.53	14.79	15.25	15.04
	14	14.99	15.58	14.35	14.34	14.55	14.81	15.27	15.06
	16	15.01	15.60	14.37	14.36	14.57	14.83	15.29	15.08

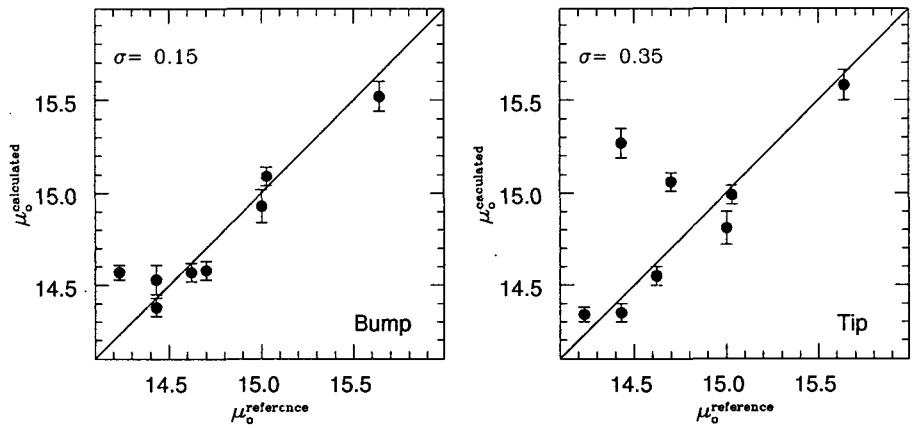

Figure 2. Comparisons of the derived distance moduli from the RGB bump (left) and tip (right) with the adopted distance moduli of eight globular clusters. The abscissa and ordinate indicate the adopted and derived distance moduli, respectively.

tance moduli of the sample clusters with those in Table 2 of Kim et al. (2006), which are adopted from Ferraro et al. (1999) and Harris (1996). Note that the adopted distance moduli of the sample clusters are basically estimated by matching the apparent brightness of the zero-age horizontal branch and to the theoretical models of Straniero et al. (1997). The standard deviations of the distance moduli derived (1) using the RGB bump are 0.34, 0.20, 0.15, and 0.20 respectively for 7, 10, 12 and 15 Gyrs, and (2) using the RGB tip are 0.35, 0.35, 0.36, and 0.37 respectively for 10, 12, 14, and 16 Gyrs. Among the considered ages, the case of 12 Gyr shows the smallest deviation. Figure 2 shows the comparison between the adopted distance and the derived distance from the RGB bump and tip, assuming the clusters' ages of 12 Gyrs. The result indicates that the near-infrared K magnitudes of the RGB bump and tip can be used to determine the distance modulus of a globular cluster in addition to the zero age-horizontal branch level with uncertainties of 0.15 and 0.35 magnitudes at a given metallicity, assuming the age of 12 Gyrs. Note that the uncertainty from the RGB tip is larger than the RGB bump by a factor of ~ 2, which may result from the ambiguity of the theoretical definition of the RGB tip and the small number statistics of brightest stars at the RGB tip.

5. CONCLUSIONS

We estimated the distance moduli of eight sample globular clusters from the apparent K magnitudes and the theoretical absolute M_K magnitudes of the RGB bump and tip. The Yonsei-Yale isochrones were used to derive the M_K magnitudes of the RGB bump and tip with respect to the cluster age and metallicity. We conclude that the near-infrared K magnitudes of the RGB bump and tip can be used to estimate the distance modulus of a globular cluster with uncertainties of 0.15 and 0.35 magnitudes.

ACKNOWLEDGEMENTS: This work was supported by the Korea Research Foundation Grant funded by the Korean Government (KRF-2005-003-C00083), for which we are grateful.

REFERENCES

Bellazzini, M., Ferraro, F. R., & Pancino, E. 2001, ApJ, 556, 635
Carreta, E. & Gratton, R. G. 1997, A&AS, 121, 95
Cho, D. -H. & Lee, S. -G. 2002, AJ, 124, 977
Ferrarese, L., Ford, H. C., Huchra, J., Kennicutt, R. C., Mould, J. R., Sakai, S., Freedman, W. L., Stetson, P. B., Madore, B. F., Gibson, B. K., Graham, J. A., Hughes, S. M., Illingworth, G. D., Kelson, D. D., Macri, L., Sebo, K., & Silbermann, N.A. 2000a, ApJS, 128, 431
Ferrarese, L., Mould, J. R., Kennicutt, R. C., Huchra, J., Ford, H. C., Freedman, W. L., Stetson, P. B., Madore, B. F., Sakai, S., Gibson, B. K., Graham, J. A., Hughes, S. M., Illingworth, G. D., Kelson, D. D., Macri, L., Sebo, K., & Silbermann, N.A. 2000b, ApJ, 529, 745
Ferraro, F. R., Messineo, M., Fusi Pecci, F., De Palo, M. A., Straniero, O., Chieffi, A., & Limongi, M. 1999, AJ, 118, 1738
Ferraro, F. R., Montegriffo, P., Origlia, L., & Fusi Pecci, F. 2000, AJ, 119, 1282
Fusi Pecci, F., Ferraro, F. R., Crocker, D. A., Rood, R. T., & Buonanno, R. 1990, A&A, 238, 95
Harris, W. E. 1996, AJ, 112, 1487
Iben, I. Jr. 1968, Nature, 220, 143
Kim, J. -W., Sohn, Y. -J., Rhee, J., Kang, A., Kim, H. -I., Kim, Y. -C., Kim, D. -G., & Chun, M. -S. 2006, submitted to A&A
Kim, Y. -C., Demarque, P., Yi, S. K., & Alexander, D. R. 2002, ApJS, 143, 499
King, C. R., Da Costa, G. S., & Demarque, P. 1985, ApJ, 299, 674
Lee, M. G., Freedman, W. L., & Madore, B. F. 1993, ApJ, 417, 553
Madore, B. F. & Freedman, W. L. 1995, AJ, 109, 1645
Rieke, G. H. & Lebofsky, M. J. 1985, ApJ, 288, 618
Schlegel, D. J., Finkbeiner, D. P., & Davis, M. 1998, ApJ, 500, 525
Straniero, O., Chieffi, A., & Limongi, M. 1997, ApJ, 490, 425
Thomas, H. -C. 1967, Z. Astrophys., 67, 420
Valenti, E., Ferraro, F. R., & Origlia, L. 2004, MNRAS, 354, 815
Valenti, E., Origlia, L., & Ferraro, F. R. 2005, MNRAS, 361, 272
Walker, A. R. 2003, in Stellar candles for the extragalactic distance scale, eds. D. Alloin & W. Gieren (New York: Springer), Lect. Notes Phys., 635, 265
Yi, S. K., Kim, Y. -C., & Demarque, P. 2003, ApJS, 144, 259
Zinn, R. J. 1985, ApJ, 293, 424